Accepted Manuscript

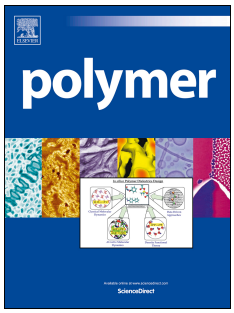

Toughness enhancement of thermosetting polymers using a novel partially reacted substructure curing protocol: A combined molecular simulation and experimental study

Changwoon Jang, Majid Sharifi, Giuseppe R. Palmese, Cameron F. Abrams

PII: S0032-3861(16)30163-X

DOI: 10.1016/j.polymer.2016.03.023

Reference: JPOL 18515

To appear in: *Polymer*

Received Date: 4 December 2015

Revised Date: 4 March 2016

Accepted Date: 7 March 2016

Please cite this article as: Jang C, Sharifi M, Palmese GR, Abrams CF, Toughness enhancement of thermosetting polymers using a novel partially reacted substructure curing protocol: A combined molecular simulation and experimental study, *Polymer* (2016), doi: 10.1016/j.polymer.2016.03.023.

For Table of Contents use only

Toughness Enhancement of Thermosetting Polymers using a Novel Partially Reacted Substructure Curing Protocol: A Combined Molecular Simulation and Experimental Study

Changwoon Jang[1], Majid Sharifi[1], Giuseppe R. Palmese[1], and Cameron. F. Abrams[1,*]

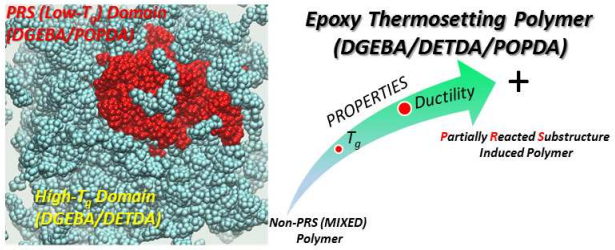

Toughness Enhancement of Thermosetting Polymers using a Novel Partially Reacted Substructure Curing Protocol: A Combined Molecular Simulation and Experimental Study

Changwoon Jang[1], Majid Sharifi[1], Giuseppe R. Palmese[1], and Cameron. F. Abrams[1,*]

[1]*Department of Chemical and Biological Engineering, Drexel University, Philadelphia, Pennsylvania 19104, United States*

ABSTRACT

Curing epoxies with a mixture of low- and high-T_g diamines has been proposed as a way to increase thermoset toughness. We seek here to understand the origins of toughness enhancement in systems comprised of the diamines poly(oxypropylene)diamine (POPDA) and diethyltoluenediamine (DETDA) together with the epoxy resin diglycidyl ether of bisphenol A (DGEBA) via control of network isomerization. Two curing protocols at constant overall DGEBA/DETDA/POPDA 2:1 amine:epoxy stoichiometric composition are compared: (i) curing a liquid mixture of DGEBA, DETDA and POPDA, and (ii) partially curing DGEBA with POPDA (60% of amines reacted), then adding DETDA and more DGEBA to continue to a fully cured stoichiometric sample; the latter is referred to as the "partially reacted substructure" (PRS) method. PRS samples are 50% tougher than the compositionally-identical mixed samples yet have higher T_g's than the mixed samples. We show here that MD simulations of model systems provide a molecular-level rationale for this observation. First, MD yields reasonably accurate densities and T_g's. Lower T_g's in the mixed systems are correlated to larger thermal fluctuations in positions of monomer centers enabled by more uniform dispersion of the POPDA molecules. Furthermore, the onset of crosslink bond stretching under steady uniaxial tensile strain occurs at lower strains in the mixed samples, which correlates to their lower experimental ductility. This

behavior is shown to arise from POPDA molecules in the PRS system more easily deforming from their unstrained conformations than they can in the mixed systems. These findings provide further guidance in the use of control over network isomerization at constant composition to enhance toughness of thermoset systems.

1. INTRODUCTION

Thermoset polymers are important synthetic materials due to their high moduli, high glass transition temperatures, and good thermal/chemical resistance [1-3]. They cure irreversibly, forming dense, stiff, highly crosslinked network structures. They are widely used in an extensive variety of applications such as matrix materials for reinforced composites [4, 5], electrical insulators [6] and adhesives [7] because of the relatively easy processing to cure by heating liquid or powder within a mold. The highly crosslinked networks, however, make these materials inherently more brittle than typical thermoplastics. Therefore, increasing fracture toughness remains an important objective of research into thermosetting polymer materials.

Conventional thermoset toughening approaches include adding elastomers or plasticizers [8-11]. Recently we demonstrated, in contrast to these additive methods, that curing protocols that allow for control of network isomerization could be used to enhance toughness at constant composition. For instance, reactive-encapsulation of inert solvent during cure followed by annealing and drying allowed the production of samples up to two-and-a-half times tougher than unmodified samples with no sacrifice in T_g or strength [12]. Another method, which we focus on here, involves the use of a blend of diamines, one of which displays a lower T_g but better ductility when used exclusively in an epoxy-based thermoset. Our major motivation here is to control the blending and curing protocol of such a dual-diamine/single-epoxy system in order to

maximize both ductility and T_g. We hypothesized that blending partially cured low-T_g diamine/epoxy with uncured high-T_g diamine and enough epoxy to guarantee a stoichiometric ratio of epoxy to amines would results in a heterogeneous microstructure that would permit a higher degree of energy dissipation under tension prior to failure than would a compositionally identical system cured from a blended monomer liquid containing all three components. We term this approach the partially reacted substructure (PRS) method. We recently demonstrated success with this approach using poly(oxypropylene)diamine (POPDA, low T_g) and diethyltoluenediamine (DETDA, high T_g) together with the epoxy resin diglycidyl ether of bisphenol A (DGEBA), with PRS samples displaying both higher fracture toughnesses and higher T_g's than fully mixed samples [13]. Despite this success, it remains somewhat unclear how the PRS method gives rise to better toughness and T_g, primarily because in the experimental systems it is essentially impossible to determine the molecular architecture and network rearrangement upon loading the amorphous crosslinked structures.

The major approach we take here is all-atom molecular dynamics (MD) simulations. MD has been used to characterize a wide range of thermoplastic and thermoset polymers and their applications at the molecular level [12, 14-18]. A key motivation for using MD in our current systems is to begin to understand the links between intra- and inter-monomer structure of network isomers and material properties. This requires that we build models of crosslinked networks with atomic resolution. We validate our structure-building approach by comparing computed densities and T_g's to experiments. We then show via analysis of positional fluctuations in the simulation trajectories why the PRS samples have higher T_g. We further show via analysis of bond-stretching why the PRS samples absorb more energy before break.

2. METHODS

2.1 Simulation Methods

Structures of DGEBA, DETDA, and POPDA are shown in Fig. 1. We used a DGEBA-DETDA/POPDA 2:1 epoxy-amine stoichiometric ratio which needs to fully reacted without any remaining reactants after 100% cure, and a diamine blend composition with 15wt% of the low-T_g diamine, realized by systems containing 400 moles of DGEBA's, 188 moles of DETDA, and 12 moles of POPDA molecules. A classical molecular dynamics code, Large-scale Atomic/Molecular Massively Parallel Simulator (LAMMPS) [19], was used as the MD engine, and the Generalized Amber force field (GAFF) [20-23] provided all interaction parameters. All MD simulations were performed using a 0.1 fs and 1 fs time step during and after generating a crosslinked network, respectively. We chose 0.1 fs time step helping the system to be stable during the ad-hoc bond create and break. The Nosé-Hoover thermostat and barostat (P = 1 bar) were applied to control the pressure and temperature.

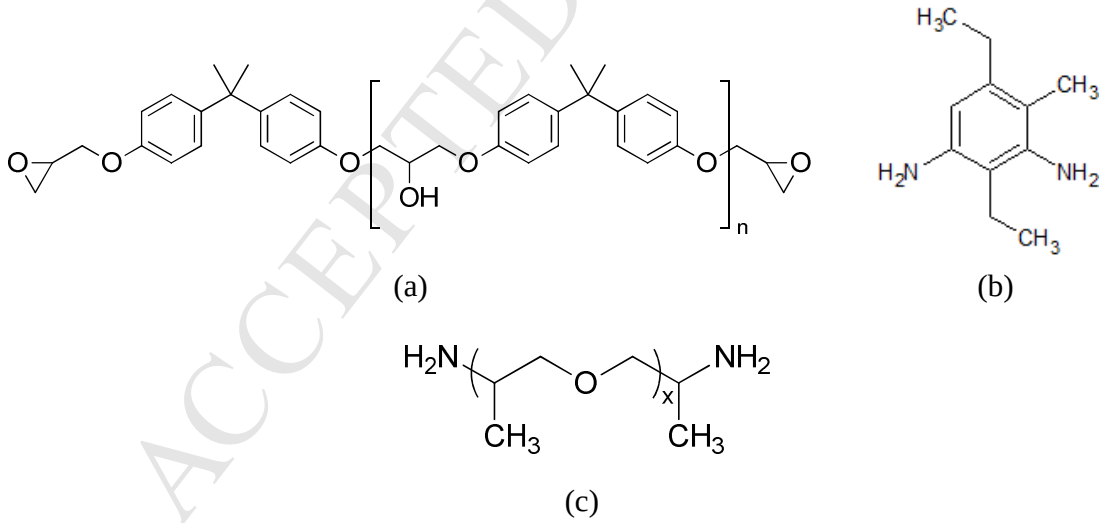

Figure 1. Chemical structures of (a) DGEBA epoxy (Miller-Stephensen) ,n=0.07, (b) DETDA (Miller-Stephensen), and (c) POPDA (Jeffamine D2000, Huntsman), x=33. A typical MD system has a composition of these three of 400:188:12.

We used a previously described curing protocol [14] to build non-PRS crosslinked samples from random liquid blends. In order to generate an isolated PRS inside the 85 wt% DGEBA/DETDA solution, liquid DGEBA/POPDA (15 wt%) was first separately equilibrated and then added to the unequilibrated liquid DGEBA/DETDA (85 wt%). The equilibrated DGEBA/POPDA was then held rigid, so the system containing DGEBA/DETDA/POPDA (including DGEBA/POPDA PRS) can be relaxed without dispersing individual molecules of DGEBA-POPDA into the DGEBA-DETDA. Then carbon-nitrogen crosslink bonds involving only POPDA nitrogens are allowed to form until 60% are cured. Then, the curing algorithm cures all remaining epoxy carbon/amine nitrogen atoms to form a 100% cured network. Figure 2 illustrates this process. Generation of the crosslinked network was performed at 600 K.

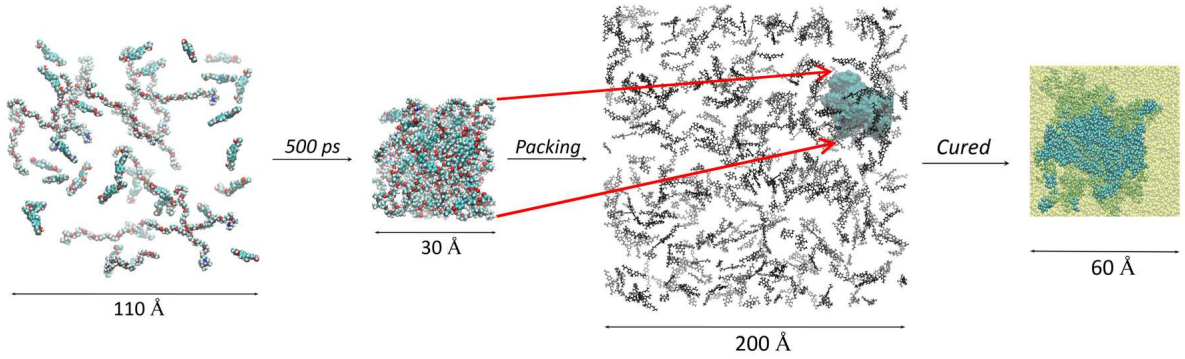

Figure 2. Generation of a PRS sample. (a) 15 wt% vapor DGEBA/POPDA at low density is condensed to (b) a liquid state. (c) The equilibrated liquid DGEBA/POPDA structure (15 wt%) is inserted into a vapor-phase DGEBA/DETDA solution (85 wt%) which is condensed and (d) then cured. Curing proceeds from this state in two stages: first, 60% cure involving only the DGEBA/POPDA crosslinking, followed by unrestricted crosslinking.

We measured the average mass densities of the systems at room temperature (300 K) after quenching the cured polymer from 600 K at which the crosslinked structures were created. The cured polymer first equilibrated for 6 ns at 600 K, then the system was cooled down to 300 K using 15 K/200ps rate at 1 bar. After cooling, the system was re-equilibrated at 300 K for another 5 ns to make sure that the system is well equilibrated at 300 K. In order to measure the glass transition temperature (T_g), the equilibrium system was cooled down from 700 K to 150 K by employing a step-wise temperature decrease of 15K/2ns cooling rate. This gives the density-temperature plot to obtain the intersection where the glass transition occurs after fitting two linear regressions in the rubbery and glassy states.

2.2 Experimental Methods

Along with the sample preparation for MD simulations, similar samples were prepared in our laboratory. Stoichiometric amounts of POPDA and DGEBA were mixed and cured at 80 °C for 15 hours. We determined the epoxy-amine chemical conversion using a Nexus FTIR spectrometer in near-IR region and by tracking the peak height corresponding to the oxirane bands at the wavenumbers of 4530 cm^{-1} [24]. Results indicated that 15 hours at 80 °C for this system is sufficient to bring the fractional conversion of epoxy-amine reactions to 60%. At this time, the mixtures were removed from the reaction conditions and cooled down to room temperature. The resulting reactive liquid samples are termed as “60% conversion PRS”. Next, we made stoichiometric blends of DGEBA and DETDA with 15 wt% PRS inclusion by weight. These batches were well mixed, degassed and cured at 80 °C for 12 hours followed by a subsequent post-curing step for 4 hours at 160 °C. The resulting cured samples were labeled as “PRS” or “PRS-modified”. Similarly, non-PRS (Mixed) blends were made by mixing the same components with the same compositions as those used in the PRS-modified samples. The three

components were well mixed and degassed without any additional pre-curing steps and cured under the same curing conditions as for the PRS-modified samples. The resulting samples were labeled as “non-PRS” or “Mixed” in this study. These two systems referred to as “polymer network isomers” due to their compositions similarities.

Three sets of experimental characterization were conducted and reported in this study. Density values were determined using water displacement technique at room temperature following the ASTM D792. The measured average density values and the associated deviations are based on at least five replicates.

Additionally, a Thermo-mechanical Analyzer TA-2940 apparatus was utilized to determine values of glass transition temperatures. Cylindrical specimens (5 mm in diameter and 5-6 mm in height) were used for this purpose. TMA measurements were conducted via a cyclic heat/cool/heat protocol with a temperature ramp rate of 2 °C/min in the temperature range of 300 K to 500 K. The reported T_g’s are based on the onset off slope change in the specific volume vs. temperature curves at the second heating cycle.

Finally, linear elastic fracture mechanics (LEFM) was used to characterize material’s toughness. Accordingly, compact tension specimens were prepared and tested under a quasi-static uniaxial extension with a crosshead speed of 1 mm/min following the ASTM D5045. The average values of strain energy release rate, G_{1c}, and the corresponding deviations were measured from at least 8 replicate per each batch.

3. RESULTS

3.1. Static Properties: Intermolecular Structure and the Glass Transition Temperature

In Table 1, we report (i) densities at 300K, as well as (ii) T_g’s computed using MD simulations along with values from experiments, and (iii) strain energy release rates.

Our prediction of densities is uniformly low but within 1% of the experimental values. T_g predictions are systematically lower but within about 3.5% of the experimental values, and the T_g of the PRS samples are higher by about 10 K. The lower T_g values compared to experimental values in this study may be due to the mismatch between the simulated and experimental structures. The experimental system has heterogeneous mixture of pre-reacted substructures but the simulated system was modeled with only a single pre-reacted substructure due to accessible system sizes. We show density vs. temperature for the simulated PRS and non-PRS systems in Fig. 3, to illustrate the method of estimating T_g from the simulations.

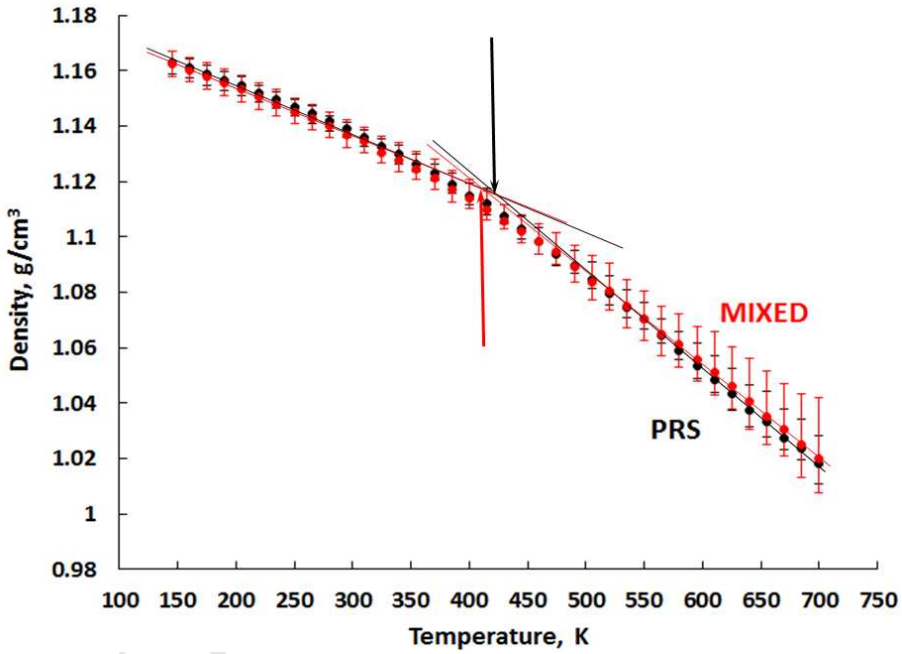

Figure 3. The glass transition temperatures for the PRS and Mixed systems.

Table 1. The densities, glass transition temperatures, and fracture energies for PRS and non-PRS systems from both experiment and simulations.

System	Density at 300K (g/cm^3)		Glass Transition Temperature (K)		Fracture Energy (kJ/m^2)
	Experiment	Simulation	Experiment	Simulation	Experiment
PRS	1.150±0.003	1.134±0.005	435±2.9	420±10.0	0.266±0.069
Mixed	1.155±0.004	1.130±0.007	425±4.3	410±12.0	0.154±0.049

It is generally thought that the glass transition temperature correlates to the uniformity of intermolecular packing and the degree of chain stiffness, because more efficiently packed and stiffer chains require more energy to activate the segmental motion necessary to enter the rubbery state [25]. Our T_g results are identical with the predicted densities of the PRS and mixed samples: the PRS samples show slightly the higher T_g, suggesting that the PRS samples reflect more efficient packing than the mixed samples. We next asked how does this manifest the higher barriers to segmental mobility the PRS samples must present? We hypothesized that this is a result of differences in nearest-neighbor intermolecular interactions between the PRS and mixed systems. First, consider that PRS samples mostly sequester the flexible POPDA molecules into the pre-reacted domains whereas, the mixed samples have more uniformly dispersed POPDA molecules. This is captured quantitatively in the methyl-methyl radial distribution function (RDF) shown in Fig. 4. Here we see, as expected, that the intramolecular packing structure of the methyls in POPDA's is insensitive to the curing protocol, while the intermolecular packing clearly shows strongly pronounced packing in the PRS samples compared to the mixed samples. This is simply because POPDA's are on average better dispersed and therefore nearest neighbors are on average farther apart in the mixed samples. We illustrate the degree of this difference using representative system snapshots showing only the methyl group carbon atoms in Fig. 5. Interestingly, we also find that the mixed systems also show a change in the packing statistics of the DETDA molecules. The RDF's for DETDA centers of mass is shown in Fig. 6. Though generally similar with a nearest-neighbor cutoff, which is the first minimum of RDF, in both systems at about 7.5 Å, we see that the number of nearest neighbors is slightly higher in the PRS system. The first coordination number, which is the number of nearest neighbors, is computed from the RDF according to

$$N = 4\pi\rho \int_0^{r_f} g(r) \cdot r^2 dr \quad (1)$$

where ρ is the number density of DEDTA centers of mass and r_f is the cutoff distance. We find N = 0.668 in the PRS systems and 0.548 in the mixed systems. We see therefore that dispersing the small amount (15 wt-% of the diamines) of POPDA alters the ordering of DETDA (the remainder of the diamines), which here happen to be much stiffer and amenable to efficient packing because of their aromaticity. In general, the amorphous structure of the PRS vs. the mixed samples qualitatively reflects the localized vs. dispersed nature, respectively, of the POPDA's. However, because POPDA's are more flexible than DETDA's, does this dispersal mean that overall segment mobility is higher in the mixed samples?

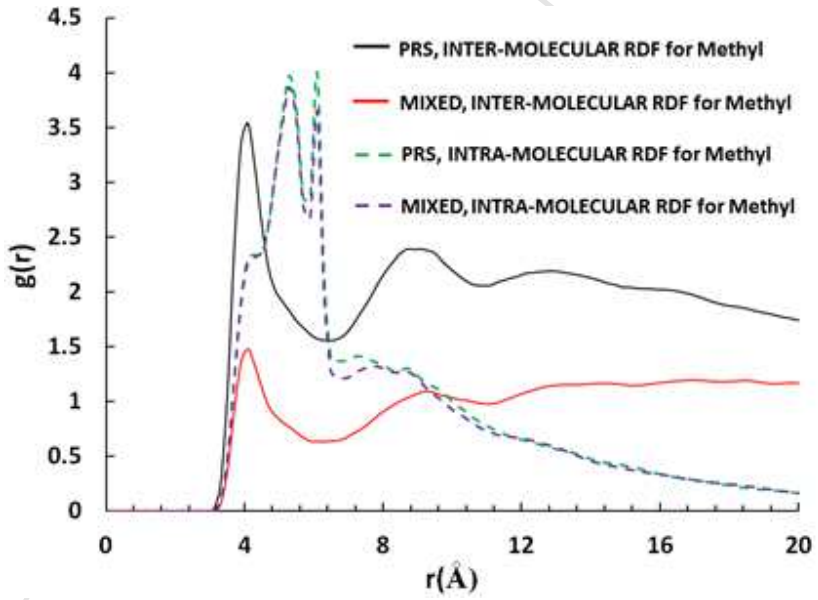

Figure 4. The inter- and intra-molecular radial distribution functions for methyl-methyl pairs of POPDA molecules.

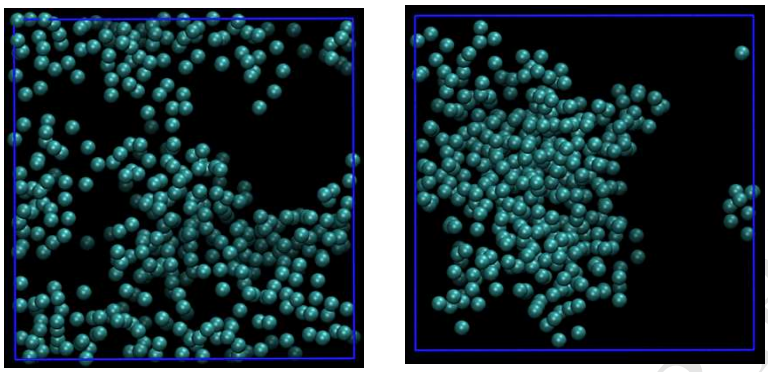

Figure 5. Representative MD system snapshots showing only POPDA methyls in the (a) mixed and (b) PRS samples. All other atom types are not shown for clarity.

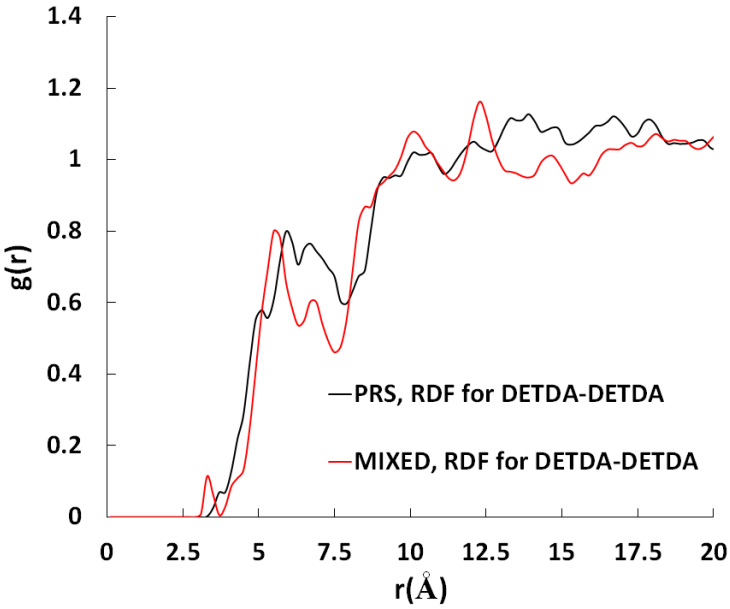

Figure 6. DETDA-DETDA RDF vs center-of-mass distance.

To answer this question, we turn to the root-mean squared fluctuations (RMSF) [26],

$$RMSF_i = \left[\frac{1}{\tau}\sum_{t_j=1}^{\tau}\left|r_i(t_j) - r_i^{ref}\right|^2\right]^{1/2} \quad (2)$$

where τ is the trajectory time over which one wants to average and r_i^{ref} is the average position of particle i over the time τ. We reasoned that the intramolecular flexibility of POPDA's is

probably not strongly dependent on whether they are localized or dispersed, and instead consider the effect of POPDA localization or dispersion on the segmental mobility of the always uniformly dispersed DGEBA molecules. Fig. 7 reports the RMSF of the isopropylidene carbons from DGEBA as a function of temperature for the PRS and mixed samples. We find that the RMSF's are generally lower in the PRS systems than in the mixed systems, with the degree of difference larger below T_g. This shows that the DGEBA molecules on average experience larger amplitude segmental motion in the mixed systems than in the PRS systems, again corroborating the observations regarding T_g. From both the static and dynamic viewpoints, it seems clear that the observed differences in T_g between PRS and mixed systems can be attributed directly to the degree of localization of the minority, more flexible, diamine: the more dispersed is the POPDA in the network, the lower the material's T_g.

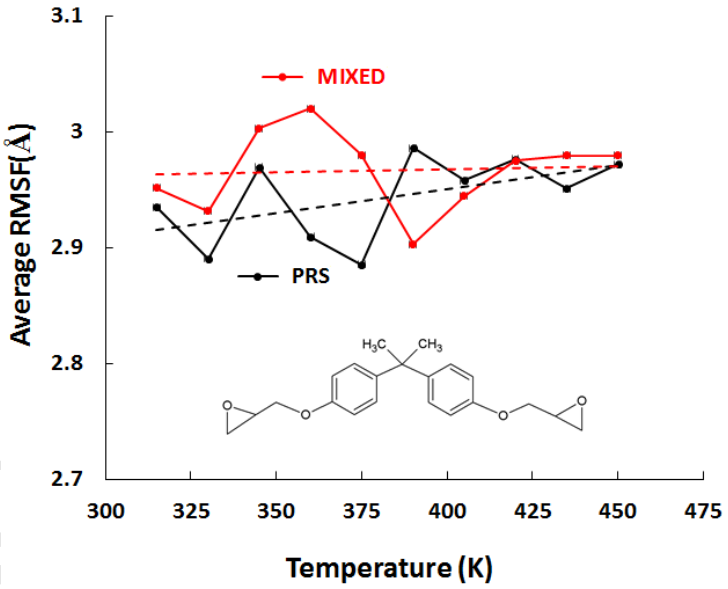

Figure 7. Root mean square fluctuations (RMSF) of the centers of mass of DGEBA molecules vs. temperature.

3.2. Correlation of cross-link bond stretching to experimental fracture toughness

Preliminary experiments as shown in Table 1 revealed that PRS samples with partial curing of 60% and a PRS mass fraction of 0.15 display fracture toughnesses more than 50% that of the compositionally identical mixed systems. The relationship between network structure and fracture toughness remains unclear. It is generally difficult to relate fracture toughness measured experimentally according to standard protocols to molecular structure, because of the complicated nature of material failure in thermoset polymers. Also, direct use of molecular simulations to measure fracture toughness is problematic because most interatomic potentials do not allow for bond breaking, and those that do remain very computationally expensive. For this reason, we sought a way to qualitatively correlate behavior in a simulated thermoset to its associated experimental fracture toughness. We reasoned that a tougher material is characterized at the molecular level as one that, when put under global uniaxial tension, has a network architecture that does a better job protecting covalent bonds from that strain than a less tough material would. That is, a tougher thermoset has a network architecture and molecular packing that allows significant slippage and rearrangement of the atomic constituents under strain before asking covalent bonds to stretch.

To test whether this hypothesis is correct, we subject our simulated systems to uniaxial strains up to 100% and tracked (1) the average length of all C-N crosslink bonds (Fig. 8a), and (2) the average -Ph-$C(CH_3)_2$-Ph- valence angle (Fig. 8b). In Fig. 9, we show the average C-N bond length as a function of axial strain, comparing three systems: (a) the PRS system, (b) the mixed system, and (c) a system in which 100% of the diamines are DETDA. Also included in the plot are subsets from the PRS and mixed systems containing data from C-N bonds in which the N is in a DETDA. There are several interesting features of these data. First, below about

30% strain, the C-N bond lengths grow very little, clearly indicating that, generally, the overall strain is not manifest in these bonds. In this regime, the network architecture is not relevant for determining the slope. However, above 30%, differences in network architecture become apparent: bond length stretching accelerates first for the mixed and pure-DETDA systems (at about 35% strain), and later for the PRS system (at about 42% strain). Clearly, the PRS systems' networks are configured such that the crosslink bonds are more effectively protected from the overall system strain. We note also that this trend remains in place if we only consider C-N bonds to the DETDA's as shown by dots in Figure 9. In Fig. 10, we show the average –Ph-C(CH3)2-Ph- valence angle as a function of uniaxial strain, and the acceleration is greater for the mixed system compared to the PRS system, again showing that the covalent structures are better protected from the global strain by the PRS systems' network architectures.

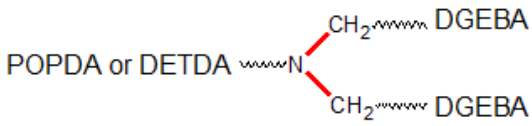

(a)

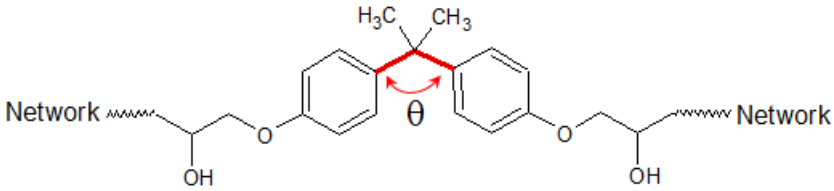

(b)

Figure 8. (a) Crosslink bonds between DGEBA and curing agents, and (b) the angle between phenyl rings on the DGEBA molecule.

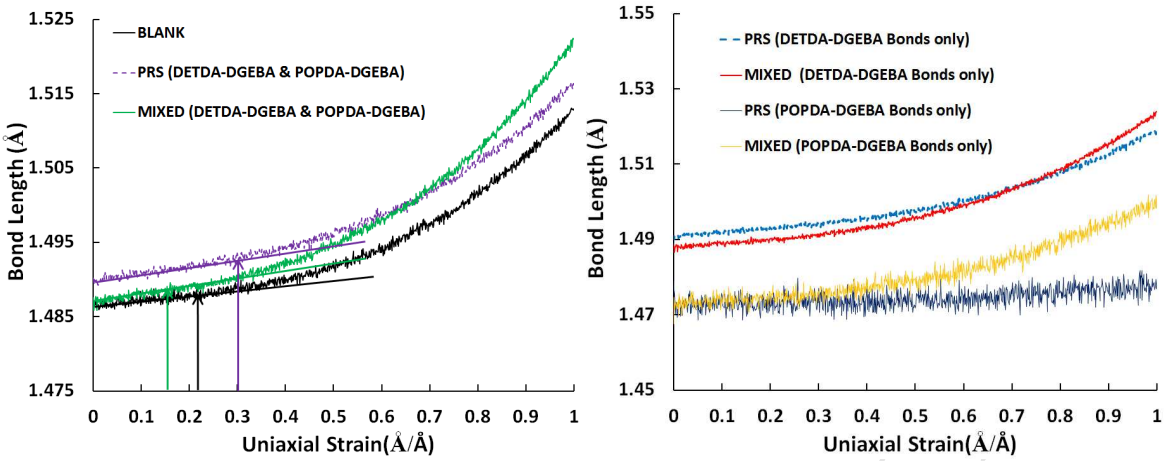

(a) (b)

Figure 9. (a) Average crosslink bond lengths vs uniaxial strain. Lines fit to the first 20% of each dataset are also drawn, and points at which the average slope of the data (fit to a 3rd order polynomial) deviates from the line by 2% are indicated with arrows. The purple and green points correspond to crosslink bonds only involving DETDA. (b) Average crosslink bond lengths covalently bonded to each curing agents (DEGBA-DETDA and DEGBA-POPDA)

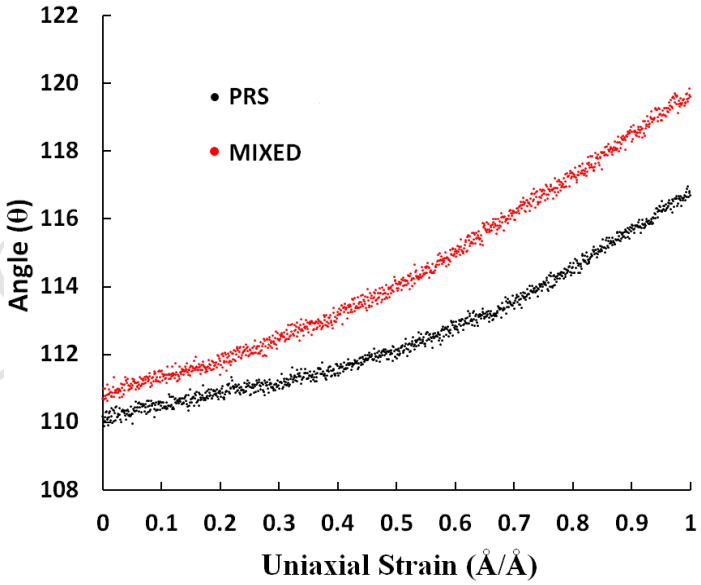

Figure 10. Average C-C-C valence angle at the isopropyl carbon of DGEBA vs. uniaxial strain

What aspect of the network architecture of the PRS systems gives rise to this property? We hypothesized that the localized POPDA's in the PRS systems form domains that are better able to absorb strain without transmitting it to the crosslink bonds than do the dispersed POPDA's in the mixed systems. The rationale for this hypothesis is that, in the blended systems, the environment around the average POPDA is more restrictive to conformational rearrangement of that POPDA than is the environment around the average POPDA in the PRS system. This would imply that, under strain, the POPDA chains in the PRS sample should deform more easily. To confirm this, we measured the end-to-end (N-to-N) distance of each POPDA chain, and we plot the average of this quantity as a function of strain for both the PRS and mixed systems in Fig. 11. Indeed, we see that the POPDA chains in the PRS samples begin to experience deformation at much earlier strains than do the POPDA chains through the packing in the PRS samples. This supports the idea that sequestering the low-T_g diamines in a homogenous in a homogenous nanodomain provides access to energy dissipation mechanisms that are absent in the mixed systems.

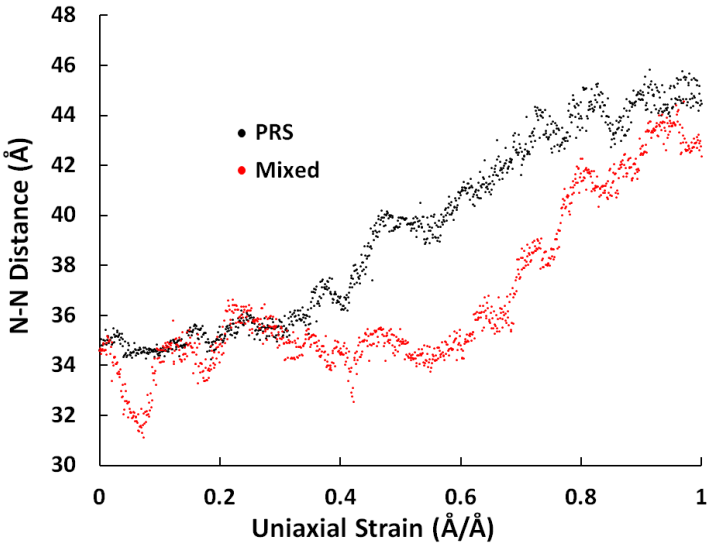

Figure 11. Average N-to-N distance of POPDA monomers vs. uniaxial strain.

4. CONCLUSION

We have used molecular simulations to explore the origins of improved T_g and fracture toughness of systems cured with the PRS method, compared to compositionally identical systems cured as uniformly dispersed mixtures. Our simulated samples display reasonable densities and T_g's compared to the experiment. We find that, because the minority diamine in the blend of diamines used in the cure is very flexible, that sequestering it as much as possible increases both T_g and resistance to bond-stretching. It improves T_g because when sequestered in a PRS region, each POPDA influences the flexibility of fewer DETDA and DGEBA molecules. We predict that the PRS method improves toughness because the PRS regions can absorb more strain before covalent bond stretching occurs than can a mixed system. These findings provide further insight into how one can improve material properties in thermoset systems at constant overall composition by careful control of network isomerization.

Acknowledgment

This work has been supported by the Cooperative Agreement between the Materials in Extreme Dynamic Environments (MEDE) Consortium and US Army Research Lab. Army Research Lab under Contract No. W911NF-12-2-0022. This work used the Extreme Science and Engineering Discovery Environment (XSEDE), which is supported by National Science Foundation grant number OCI-105375 (allocation TG-MCB070073N) and US Air Force Research Laboratory-DOD Supercomputing Resource Center Environment (AFRL DSRC) (allocation ARLAP35100034).

REFERENCES

[1] C.A. May, Epoxy resins chemistry and technology, second ed., Marcel Dekker, New York, 1987.

[2] The Epoxy Book, System Three Resins, Inc., Auburn, Washington, USA, 2001. https://cdn.shopify.com/s/files/1/1000/1906/files/The_Epoxy_Book.pdf, (accessed 15.12.03).

[3] H. Lee, K. Neville, Handbook of Epoxy Resins. McGraw-Hill, New York, 1982.

[4] J.J. Morena, Advanced Composite Mold Making, Van Nostrand Reinhold Co Inc, New York, 1988.

[5] J. Njuguna, K. Pielichowski, J.R. Alcock, Epoxy-based fibre reinforced nanocomposites, Adv. Eng. Mater. 9(2007) 835-847.

[6] E. Tuncer, I. Sauers, D.R. James, A.R. Ellis, M.P. Paranthaman, T. Aytug, S. Sathyamurthy, K.L. More, J. Li, A. Goyal, Electrical properties of epoxy resin based nano-composites, Nanotechnology, 18(2007) 025703(6pp).

[7] C.F. Carlborg, A. Vastesson, Y. Liu, W.van der. Wijngaart, M. Johansson, T. Haradldsson, Functional off-stoichiometry thiol-ene-epoxy thermosets featuring temporally controlled curing stages via an UV/UV dual cure process, J. Polym. Sci. A Polym. Chem, 52(2014) 2604-2615.

[8] R.S. Drake, A.R. Siebert, Elastomer-modified epoxy resins for structural applications, SAMPE Q. 6(1975) 11-21.

[9] R. Bagheri, B.T. Marouf, R.A. Pearson, Rubber-toughened epoxies: A critical review, Polym. Rev. 49(2009) 201-225.

[10] J.N. Sultan, F.J. McGarry, Microstructural Characteristics of Toughened Thermoset Polymers. MIT School of Engineering Report 1969, R69-59.

[11] J.N. Sultan, F.J. McGarry, Effect of rubber particle size on deformation mechanisms in glassy epoxy, Polym. Eng. Sci. 13(1973) 29-34.

[12] M. Sharifi, C. Jang, C.F. Abrams, G.R. Palmese, Toughened epoxy polymers via rearrangement of network topology, J. Mater. Chem. A. 2(2014) 1601-16082.

[13] M. Sharifi, C. Jang, C.F. Abrams, G.R. Palmese, Epooxy polymer networks with improved thermal and mechanical properties via controlled dispersion of reactive toughening agent, Macromolecules, 48(2015) 7495-7502.

[14] C. Jang, M. Sharifi, G.R. Palmese, C.F. Abrams, Crosslink network rearrangement via reactive encapsulation of solvent in epoxy curing: A combined molecular simulation and experimental study, Polymer, 55(2014) 3859-3868.

[15] P.V. Komarov, C. Yu-Tsung, C. Shih-Ming, P.G. Khalatur, P. Reineker, Highly Cross-linked epoxy resins: An atomistic molecular dynamics simulation combined with a mapping/reverse mapping procedure, Macromolecules, 40(2007) 8104-8113.

[16] J. Gou, B. Minaie, B. Wang, Z. Liang, C. Zhang, Computational and experimental study of interfacial bonding of single-walled nanotube reinforced composites, Comp. Mater. Sci. 31(2004) 225-236.

[17] Y. Li, Y. Liu, X. Peng, C. Yan, S. Liu, N. Hu, Pull-out simulations on interfacial properties of carbon nanotube-reinforced polymer nanocomposites, Comp. Mater. Sci. 50(2011) 1854-1860.

[18] K. Liao, S. Li, Interfacial characteristics of a carbon nanotube-polystyrene composite system, Appl. Phys. Lett. 79(2001) 4225-4227.

[19] S. Plimpton, Fast parallel algorithms for short-range molecular dynamics, J. Comput. Phys. 117(1995) 1-19.

[20] J. Wang, R.M. Wolf, J.W. Caldwell, P.A. Kollman, D.A. Case, Development and testing of a general amber force field, J. Comput. Chem. 25(2004) 1157-1174.

[21] J. Wang, W. Wang, P.A. Kollman, D.A. Case, Automatic atom type and bond type perception in molecular mechanical calculations, J. Mol. Graph. Model. 25(2006) 247-260.

[22] A. Jakalian, D.B. Jack, C.I. Bayly, Fast, efficient generation of high-quality atomic charges. AM1-BCC model: I. Method J. Comput. Chem. 21(2000) 132-146.

[23] A. Jakalian, D.B. Jack, C.I. Bayly, Fast, efficient generation of high-quality atomic charges. AM1-BCC model: II. Parameterization and validation, J. Comput. Chem. 23(2002) 1623-1641.

[24] J. Mijovic, S. Andjelic, A study of reaction kinetics by near-infrared spectroscopy. 1. Comprehensive analysis of a model epoxy/amine system, Macromolecules, 28(1995) 2787-2796.

[25] K. Kunal, C.G. Robertson, S. Pawlus, S.F. Hahn, A.P. Sokolov, Role of chemical structure in fragility of polymers: A qualitative picture, Macromolecules, 41(2008) 7232-7238.

[26] N.C. Benson, V. Daggett, Dynameomics: large-scale assessment of native protein flexibility, Protein Sci. 17(2008) 2038-2050.

Table of Contents use only

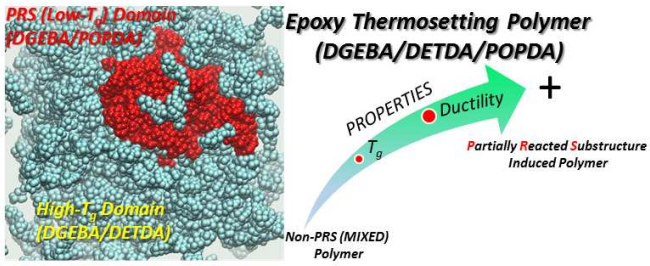

Highlights

- Molecular simulations and experiments of DGEBA/DETDA/POPDA thermosets.
- Partially-reacted substructures (PRS) of DGEBA/POPDA enhance toughness.
- Toughness enhancement occurs via conformational relaxation in PRS domains.